Decentralized Energy Management of Microgrid Based on Blockchain-Empowered Consensus Algorithm with Collusion Prevention

Hongyi Li, *Student Member, IEEE,* Hongxun Hui, *Member, IEEE,* Hongcai Zhang, *Senior Member, IEEE*

***Abstract*—The concern for privacy and scalability has motivated a paradigm shift to decentralized energy management methods in microgrids. The absence of a central authority brings significant challenges to promote trusted collaboration and avoid collusion. To address these issues, this paper proposes a blockchain-empowered microgrid energy management framework, which adopts a novel consensus-based algorithm with a collusion prevention mechanism. Aiming at social welfare maximization, the energy management problem is formulated into a convex and decomposable form, which can be solved in a decentralized manner. To prevent the collusion between malicious agents, we propose a random information transmission mechanism empowered by the blockchain smart contract to replace the time-invariant communication topology. The consensus-based algorithm is extended to obtain the optimal solution of the energy management problem on the random and time-varying communication topology. We theoretically proved that the proposed algorithm converges to the global optimal solution with a probability of 1, without violating the physical constraints of individual agents. The effectiveness of the proposed method was validated by multiple experiments, both within the simulation environment and on a hardware system.**

***Index Terms*—blockchain-based optimization, consensus algorithm, decentralized energy management, time-varying digraph.**

NOMENCLATURE

Indexes

i	Index of agents.
k	Index of iterations.

Sets

$\mathcal{I}$	Set of all agents in the microgrid.
$\mathcal{I}_{\mathrm{L}}$	Set of flexible loads.
$\mathcal{I}_{\mathrm{G}}$	Set of dispatchable generators.
$\mathcal{I}_{\mathrm{R}}$	Set of renewable energy sources.
$\mathcal{N}_i^-$	Set of out-neighbors of agent i.
$\mathcal{N}_i^+$	Set of in-neighbors of agent i.
$\mathcal{V}$	Set of nodes in the graph.
$\mathcal{E}$	Set of activated links.

Variables

λ	Lagrangian dual variable.
λ_i	Price estimation of agent i.
ζ	Global power mismatch.
ζ_i	Local power mismatch estimation of agent i.
P_i	Power generation/consumption of agent i.

Parameters

δ_k	Euclidean distance to the global optimum at iteration k.
η	Step size of updating the dual variable.
ϵ_λ	Convergence threshold for λ_i.
ϵ_ζ	Convergence threshold for ζ_i.
π_i	Welfare of agent i.
π	Welfare of the microgrid.
ρ_i	Percentage difference of the power schedule of agent i compared with the optimal solution.
ϱ_i	Percentage difference of the price estimation of agent i compared with the optimal solution.
b_{ij}	Weight of the power mismatch estimation sent from agent j to agent i.
$C_i(\cdot)$	Generation cost function of generator i.
$\mathcal{G}$	Communication topology.
l_i	Coefficient of the linear term of the cost/utility function of agent i.
P_i^{max}	Upper limit of power of agent i.
P_i^{min}	Lower limit of power of agent i.
ΔP_i	Change of the power schedule of agent i between two iterations.
q_i	Coefficient of the quadratic term of the cost/utility function of agent i.
$U_i(\cdot)$	Utility function of load i.
w_{ij}	Weight of the electricity price estimation sent by agent j to agent i.

I. INTRODUCTION

THE decarbonization of the power system has motivated the prevalence of distributed renewable energy sources (RESs) [1]. As onsite generators, the electricity generated by distributed RESs can be accommodated locally to reduce the transmission cost [2]. However, the intermittent and stochastic nature of RESs poses significant challenges to the operation of the grid [3], [4]. Providing an interconnection to dispatchable generators and flexible loads, the microgrid has been widely

This paper is funded in part by the Science and Technology Development Fund, Macau SAR (File no. SKL-IOTSC(UM)-2021-2023, and File no. 0003/2020/AKP) and in part by the Zhuhai Science and Technology Innovation Bureau (File no. ZH22017002210007PWC). (Corresponding author: *Hongcai Zhang*.)

H. Li, H. Hui, and H. Zhang are with the State Key Laboratory of Internet of Things for Smart City and Department of Electrical and Computer Engineering, University of Macau, Macao, 999078 China (email: hczhang@um.edu.mo).

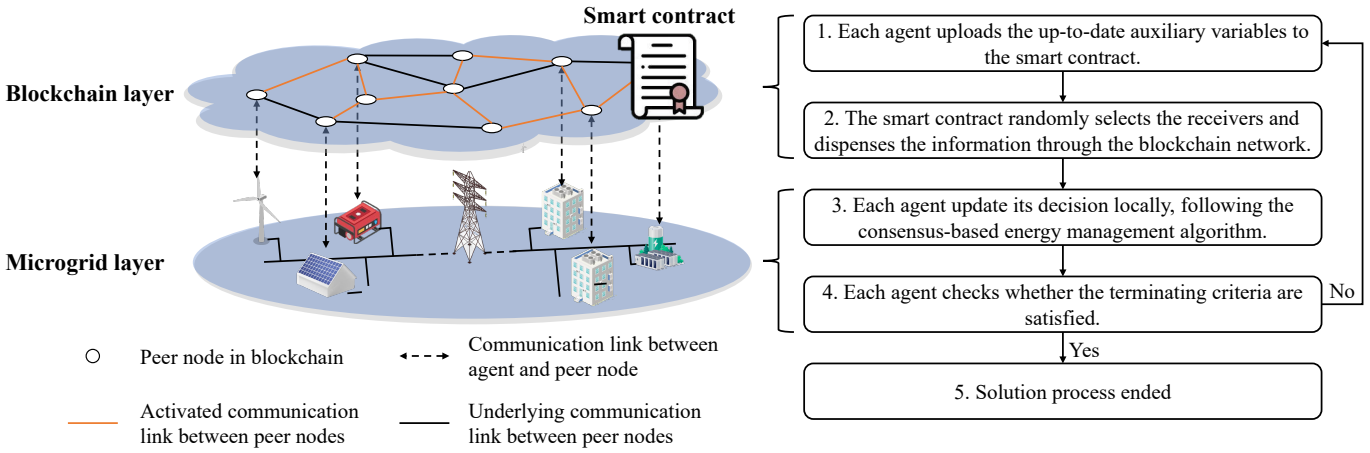

Fig. 1. Illustration of the proposed blockchain-empowered microgrid energy management framework based on consensus algorithm. The blockchain layer consists of peer nodes, which hold the distributed ledger and the smart contract. The microgrid layer consists of RESs, diesel generators, and flexible loads, which are called agents. To prevent collusion, the information exchange between agents is achieved by a smart contract through the blockchain network. The agents upload their auxiliary variables to the smart contract every iteration. The smart contract randomly selects the receivers and dispenses the information through the blockchain network. After exchanging information, each agent updates its decision locally, following the consensus-based energy management algorithm. Thereby, the microgrid energy management problem is solved in a collective way.

adopted to promote the local accommodation of RES generation [5].

Toward the optimal coordination of RESs, dispatchable generators, and flexible loads, the energy management of microgrids has become an active research topic [6]. Some researchers have proposed centralized energy management algorithms to utilize different kinds of flexible resources. Kanchev *et al.* [7] proposed a microgrid energy management algorithm to dispatch small-scale gas turbines with distributed RESs. Parisio *et al.* [8] and Arkhangelski *et al.* [9] designed energy management algorithms that utilize flexible loads to mitigate the fluctuations of RES generation. Although the above-mentioned energy management algorithms promote the local accommodation of RES generation in microgrids, these centralized methods have critical disadvantages such as privacy issues, the single point of failure problem, and low scalability.

With the digitalization of the power system, applying distributed algorithms on a multi-agent system for energy management has become a vibrant research area [10]. The consensus-based algorithm is a popular approach to achieve fully decentralized coordination of multiple agents, as it eliminates the need for a central coordinator and only requires neighboring communication [11]. Researchers have applied consensus-based algorithms to both bidirectional and unidirectional communication topologies. Rahbari-Asr *et al.* [12] developed an incremental welfare consensus algorithm for energy management with bidirectional communication, aiming at social welfare maximization. Zhao *et al.* [13], [14] focused on unidirectional communication and proposed consensus algorithms to tackle the transmission loss and enhance privacy protection. Hui *et al.* [15] studied the optimal coordination of diesel generators and flexible loads with high plug-and-play expandability. The above-mentioned research assumed that the communication networks were ideal and fixed. However, in real-world implementations, random link failures and congestion always occur, which has motivated research on consensus algorithms over random and time-varying communication topologies [16]. Wu *et al.* [17] extended the consensus-based algorithm considering random packet drops in the communication network. Yang *et al.* [18] studied the consensus algorithm over communication networks with stochastic noise. Modeling the status of the communication network as a Bernoulli process, Wang *et al.* [19] implemented a gossip-based consensus algorithm for energy management with random link failures. Zhao *et al.* [20] studied the optimal resource management in the microgrid, considering single link/node failure in the network. However, there still exist two challenges that have not been properly addressed in the published literature: 1) the decentralized optimization problem requires a trusted and verifiable solution environment, and 2) malicious agents might collude and cheat.

Blockchain is a distributed ledger technology with the features of transparency, verifiability, and immutability [21]. Different from a centralized database, in a blockchain network, the data and update are transparent, since each node in the network maintains a copy of the ledger. The ledger consists of sequential information linked by cryptography, which enables the nodes to verify the correctness of the data [22]. The application of blockchain in the smart grid has been explored by researchers. Luo *et al.* [23] proposed a blockchain-based platform for trusted data aggregation and power dispatch in the microgrid. Yang *et al.* [24] developed a blockchain-based transactive energy system for residential prosumers, which allowed verifiable transaction recording and preserved user privacy. The advent of blockchain smart contracts further empowers the automatic execution of predetermined functions. Using the smart contract, the solving of energy management problems can be achieved within the blockchain network, making the solution process verifiable and reliable. Luo *et*

al. [25] designed a blockchain-based transaction settlement mechanism for the peer-to-peer energy sharing within prosumer coalitions. Di Silvestre *et al.* [26] proposed an energy blockchain framework that optimally scheduled the power in the microgrid. Leeuwen *et al.* [27] and Yang *et al.* [28] solved the energy management problem with the alternating direction method of multipliers (ADMM). The smart contract was utilized to act as the central coordinator, which solved the dual problem of the ADMM. However, the solution of the dual problem of the ADMM requires the smart contract to collect information from all nodes. The task of solving the dual problem can be assigned to a single node, e.g., in Reference [27], while this node might suffer from some critical issues, such as a high computational burden. If multiple nodes solve the dual problem in parallel, it might lead to a waste of computational resources. Instead of directly solving the dual problem, the consensus-based algorithms work with neighboring information exchange between agents [29]. At each iteration, with the information from its neighborhood, each agent locally updates its decision until consensus is reached. Because there is no need to collect information from all of the agents, the consensus-based algorithm could be a better candidate for implementation in the decentralized blockchain network. To the best of the authors' knowledge, blockchain-empowered optimization based on fully decentralized consensus-based algorithms has not been reported in the literature.

Previous research usually assumed that the agents were honest and exchanged information with their neighbors following consensus-based algorithms [30]. However, there may be malicious agents that may collude and send manipulated information to an innocent agent when the communication topology is fixed and known [31], [32]. By misleading the decision of innocent agents with manipulated information, malicious agents benefit, while the interests of the innocent agents are compromised. Such collusion is difficult to detect, since the physical constraints of the system are not violated. Chen *et al.* [33], [34] proposed a blockchain-based approach to detect collusion in energy management, by selecting a few delegates from the agents to form a coordination committee. This approach assumes that the majority of the committee is honest, while it might fail if the malicious agents take the majority in the committee. Because malicious agents rely on a fixed and known communication topology to design the manipulated information, the collusion can also be effectively prevented if the communication topology becomes random and unknown *a priori*. However, the communication networks used in consensus-based methods are usually sparse, making it difficult to randomize the communication topology. With the blockchain smart contract, the receivers of the information can be randomly selected, which forms a communication topology that is unknown *a priori*. Thus, the collusion can be effectively prevented. To the best knowledge of the authors, related communication mechanisms and blockchain frameworks have not been reported in the literature.

In this paper, we propose a blockchain-empowered framework to solve the energy management problem of microgrids with the consensus-based algorithm. Instead of letting the agents communicate with each other directly, the smart contract is utilized to forward the information from one agent to several randomly selected receivers, and thereby the malicious agents cannot find their accomplices and the collusion is prevented. The randomness of the communication topology brings significant challenges to guarantee the convergence of the consensus-based algorithm and the optimality of the obtained solution. To tackle this issue, we adopt a novel consensus-based algorithm and theoretically prove the effectiveness of the algorithm over the proposed communication mechanism. The contributions of this paper are threefold:

1) A blockchain framework is proposed for the energy management in microgrids. The coordination of the RESs, the diesel generators, and the flexible loads are modeled as a convex and decomposable problem, which is solved by a blockchain-based decentralized algorithm.
2) To prevent collusion, we propose a random information transmission mechanism based on a blockchain smart contract to replace the conventional time-invariant communication topology. The consensus-based algorithm is extended to solve the energy management problem over the random and time-varying communication topology.
3) Based on matrix perturbation theory and the Karush–Kuhn–Tucker (KKT) conditions, we theoretically prove that over the time-varying communication topology, the proposed algorithm converges to the global optimal solution with probability 1, and the physical constraints of individual agents are not violated.

The remainder of this paper is organized as follows. Section II introduces the proposed blockchain framework and the model of the energy management problem. Section III presents the design of the consensus-based energy management algorithm and the theoretical proofs of its effectiveness. Section IV demonstrates the effectiveness of the proposed method through numerical case studies. Section V concludes the paper.

II. Preliminary Models

A. Blockchain-Empowered Energy Management Framework

As shown in Fig. 1, we propose a blockchain-empowered microgrid energy management framework that consists of two layers, namely the blockchain layer and the microgrid layer. The blockchain layer is based on an open-source permissioned blockchain framework, Hyperledger Fabric [35]. The microgrid layer consists of RESs, diesel generators, and flexible loads, which are referred to as agents in the following discussions. In the proposed framework, each agent in the microgrid holds a peer node, which is the basic component of the blockchain layer. With the peer node, each agent maintains a copy of the blockchain. As the solution process of the energy management problem is recorded in the blockchain, any malicious manipulations of information can be traced. Thus, a trusted and verifiable solution environment is established between agents in the microgrid.

The blockchain smart contract is utilized to enable the automatic operation of the blockchain layer. The agents can only interact with the blockchain by invoking the pre-defined functions in the smart contract, which is installed on the peer

node. As previously discussed, in conventional consensus-based algorithms, the agents usually exchange information through a known and fixed communication topology. When the communication topology is fixed and known, malicious agents can collude and send manipulated information to specific receivers to mislead their decision. To tackle this issue, we integrate a random information transmission module into the smart contract to prevent collusion. At each iteration, the agents upload the information to the smart contract. The smart contract randomly selects the receivers and dispenses the information through the blockchain network. In this way, a time-varying communication topology between agents is formed, where the receivers are unknown to the senders *a priori*. With the communication topology being random and time varying, the malicious agents cannot collude as they cannot identify the receivers of their information.

We further design a consensus-based algorithm, which is introduced in detail in Section III, for the decentralized solution of the energy management problem. Exchanging only auxiliary variables, each agent updates its power schedule locally. Thus, private information, e.g., cost functions and power limits, are well-protected from leaking. Through an iterative process, the agents solve the energy management problem collectively. Therefore, with the proposed blockchain framework and the consensus-based energy management algorithm, we provide a trusted and verifiable environment to solve the energy management problem in a privacy-protecting and collusion-preventing manner.

B. Optimization Problem Formulation

This subsection formulates the optimal energy management problem that will be solved by the proposed blockchain framework. Before that, we first define the necessary notation here. Three sets are defined to categorize the agents, namely the set of RESs $\mathcal{I}_{\mathrm{R}}$, the set of diesel generators $\mathcal{I}_{\mathrm{G}}$, and the set of flexible loads $\mathcal{I}_{\mathrm{L}}$. The set of all of the agents is defined as the union of three sets, i.e., $\mathcal{I} = \mathcal{I}_{\mathrm{R}} \cup \mathcal{I}_{\mathrm{G}} \cup \mathcal{I}_{\mathrm{L}}$. Using k as the iteration index, the time-varying communication topology of the multi-agent system is represented by a directed graph $\mathcal{G}(k) = \{\mathcal{V}, \mathcal{E}(k)\}$. The node set $\mathcal{V}$ is equivalent to the agent set $\mathcal{I}$. The edge set $\mathcal{E}(k)$ represents the activated communication links between agents, which vary across iterations. An edge $(i,j) \in \mathcal{E}(k)$ means that agent i receives information from agent j at iteration k. The set of out-neighbors of agent i at iteration k is defined as $\mathcal{N}_i^-(k) = \{j | (j,i) \in \mathcal{E}(k),\ i \neq j\}$. Similarly, the set of in-neighbors of agent i at iteration k is defined as $\mathcal{N}_i^+(k) = \{j | (i,j) \in \mathcal{E}(k),\ i \neq j\}$. Digraph $\mathcal{G}(k)$ is assumed to be a simple graph, i.e., multiple edges and self-loops are not considered. With the price of electricity in one market interval denoted as λ, the optimization models of individual agents in the microgrid are outlined below.

1) Model of Renewable Energy Sources: Assuming that the renewable energy generation has no cost, the objective of the RES is to maximize the profit of electricity generation within its predicted generation. For each RES $i \in \mathcal{I}_{\mathrm{R}}$, its individual optimization problem can be written as

$$\begin{aligned} \min_{P_i} \quad & -\lambda P_i \\ \text{s.t.} \quad & 0 \le P_i \le P_i^{\max}, \end{aligned} \tag{1}$$

where P_i is the actual power generation of RES i, and $P_i^{\max}$ is its predicted maximum available power generation.

2) Model of Diesel Generators: For each diesel generator $i \in \mathcal{I}_{\mathrm{G}}$, its generation cost function $C_i(P_i)$ can be represented by a quadratic function of its power output P_i [12], [36]:

$$C_i(P_i) = q_i P_i^2 + l_i P_i,\ \forall i \in \mathcal{I}_{\mathrm{G}}, \tag{2}$$

where q_i and l_i are coefficients of the quadratic term and linear term, respectively. Then, for diesel generator $i \in \mathcal{I}_G$, the individual optimization problem can be written as

$$\begin{aligned} \min_{P_i} \quad & C_i(P_i) - \lambda P_i \\ \text{s.t.} \quad & P_i^{\min} \le P_i \le P_i^{\max}, \end{aligned} \tag{3}$$

where $P_i^{\min}$ and $P_i^{\max}$ are the lower and upper bounds of its power generation, respectively.

3) Model of Flexible Loads: For each flexible load $i \in \mathcal{I}_{\mathrm{L}}$, we define a utility function, $U_i(P_i)$, in units of \$, to describe its satisfaction of consuming electricity. The utility function $U_i(P_i)$ is assumed to have the following properties [14], [37]:

1) Non-decreasing: The utility function is a non-decreasing function with respect to the power consumption P_i, i.e., $\frac{\partial U_i(P_i)}{\partial P_i} \ge 0$;
2) Saturation: The second-order derivative of the utility function is non-positive, i.e., $\frac{\partial^2 U_i(P_i)}{\partial P_i^2} \le 0$;
3) Zero-crossing: The utility is zero when there is no electricity consumption, i.e., $U_i(0) = 0$.

An example of the utility function that satisfies the above conditions is a quadratic function [12], [13]:

$$U_i(P_i) = q_i P_i^2 + l_i P_i, \tag{4}$$

where q_i and l_i are the coefficients of the quadratic term and linear term, respectively, satisfying

$$2 q_i P_i^{max} + l_i = 0,\ q_i < 0,\ l_i > 0, \tag{5}$$

which ensures that the utility function saturates at the maximum power consumption. For flexible load $i \in \mathcal{I}_L$, the objective is to minimize its electricity purchase costs minus its utility, which can be formulated as

$$\begin{aligned} \min_{P_i} \quad & \lambda P_i - U_i(P_i) \\ \text{s.t.} \quad & P_i^{\min} \le P_i \le P_i^{\max}, \end{aligned} \tag{6}$$

where $P_i^{\min}$ and $P_i^{\max}$ are the lower and upper bounds of the power consumption, respectively.

4) Microgrid Energy Management Problem: The goal of energy management is to maximize the social welfare. Thus, combining the optimization problems of individual agents, the energy management problem of the microgrid is modeled as

$$\min_{P_i,\ i \in \mathcal{I}} \quad \sum_{i \in \mathcal{I}_{\mathrm{G}}} C_i(P_i) - \sum_{i \in \mathcal{I}_{\mathrm{L}}} U_i(P_i) \tag{7a}$$

$$\text{s.t.} \quad \sum_{i \in \mathcal{I}_{\mathrm{R}}} P_i + \sum_{i \in \mathcal{I}_{\mathrm{G}}} P_i - \sum_{i \in \mathcal{I}_{\mathrm{L}}} P_i = 0, \tag{7b}$$

$$P_i^{\min} \le P_i \le P_i^{\max},\ \forall i \in \mathcal{I}. \tag{7c}$$

It is assumed that the following relationship holds

$$\sum_{i\in\mathcal{I}_{\mathrm{R}}\cup\mathcal{I}_{\mathrm{G}}} P_i^{\min} \leq \sum_{i\in\mathcal{I}_{\mathrm{L}}} P_i^{\min} < \sum_{i\in\mathcal{I}_{\mathrm{L}}} P_i^{\max} \leq \sum_{i\in\mathcal{I}_{\mathrm{R}}\cup\mathcal{I}_{\mathrm{G}}} P_i^{\max}, \tag{8}$$

which ensures that the flexible loads can be supplied by the generators, i.e., problem (7) has a feasible solution.

III. Proposed Consensus-Based Energy Management Algorithm

A. Design of Consensus-Based Algorithm

Given that problem (7) is convex and strong duality holds, the consensus-based algorithm is formulated on the basis of the classical primal-dual decomposition method [38]. The equality constraint (7b) is written into the objective function as follows:

$$\begin{aligned}\mathcal{L}\left(\boldsymbol{P},\lambda\right) = &\sum_{i\in\mathcal{I}_{\mathrm{G}}} C_i(P_i) - \sum_{i\in\mathcal{I}_{\mathrm{L}}} U_i(P_i) \\ &+ \lambda\left(\sum_{i\in\mathcal{I}_{\mathrm{L}}} P_i - \sum_{i\in\mathcal{I}_{\mathrm{G}}} P_i - \sum_{i\in\mathcal{I}_{\mathrm{R}}} P_i\right),\end{aligned} \tag{9}$$

where λ is the Lagrange multiplier, which is interpreted as the electricity price in the context of energy management.

Since the inequality constraints (7c) are local constraints of the agents, given $\lambda\left(k+1\right)$, for individual agents, their power schedules can be updated by solving the sub-problems

$$P_i\left(k+1\right) = \begin{cases} \underset{P_i}{\text{argmin}} \ -\lambda\left(k+1\right)P_i \\ \quad \text{s.t. } 0 \leq P_i \leq P_i^{\max} & ,\forall i\in\mathcal{I}_{\mathrm{R}}, \\ \underset{P_i}{\text{argmin}} \ C_i(P_i) - \lambda\left(k+1\right)P_i \\ \quad \text{s.t. } P_i^{\min} \leq P_i \leq P_i^{\max} & ,\forall i\in\mathcal{I}_{\mathrm{G}}, \\ \underset{P_i}{\text{argmin}} \ \lambda\left(k+1\right)P_i - U_i(P_i) \\ \quad \text{s.t. } P_i^{\min} \leq P_i \leq P_i^{\max} & ,\forall i\in\mathcal{I}_{\mathrm{L}}. \end{cases} \tag{10}$$

Given the solutions of the sub-problems, the Lagrange multiplier λ can be updated along its gradient direction, which is called solving the master problem, as follows:

$$\lambda\left(k+1\right) = \lambda\left(k\right) + \eta\zeta\left(k\right), \tag{11}$$

$$\zeta\left(k\right) = \left(\sum_{i\in\mathcal{I}_{\mathrm{L}}} P_i\left(k\right) - \sum_{i\in\mathcal{I}_{\mathrm{G}}} P_i\left(k\right) - \sum_{i\in\mathcal{I}_{\mathrm{R}}} P_i\left(k\right)\right), \tag{12}$$

where η is the step size, and $\zeta\left(k\right)$ is the mismatch between the power consumption and generation.

The classical primal-dual decomposition method iteratively solves the above master and sub-problems, and it converges to an optimal solution in finite iterations. However, in equations (11) and (12), the calculation of λ and ζ requires collecting information from all agents, which is unavailable to individual agents in a decentralized solution process. Thus, we introduce two consensus variables, λ_i and ζ_i, to represent the local estimation of the global information performed by agent i. We also introduce two matrices, namely, $\boldsymbol{W}\left(k\right) = \left[w_{ij}\left(k\right)\right]$ and $\boldsymbol{B}\left(k\right) = \left[b_{ij}\left(k\right)\right]$, to weight λ_i and ζ_i at each iteration, respectively. Since our proposed method adopts a time-varying communication topology, the weight matrices need to vary across iterations. Inspired by References [13], [18], [19], we define the weights as

$$w_{ij}\left(k\right) = \begin{cases} \frac{1}{\left|\mathcal{N}_i^+(k)\right|+1}, & \forall j\in\mathcal{N}_i^+\left(k\right) \\ 0, & \text{otherwise} \end{cases}, \tag{13}$$

$$b_{ij}\left(k\right) = \begin{cases} \frac{1}{\left|\mathcal{N}_i^-(k)\right|+1}, & \forall j\in\mathcal{N}_i^-\left(k\right) \\ 0, & \text{otherwise} \end{cases}, \tag{14}$$

where $\left|\cdot\right|$ denotes the cardinality of the set.

The proposed consensus algorithm is outlined in Algorithm 1. According to equation (13), for agents $j\in\mathcal{N}_i^+(k)$, the weights $w_{ij}(k)$ are equal and sum to 1, implying that the first two terms of equation (17) calculate the weighted average of $\lambda_j, j\in\mathcal{N}_i^+(k)$. In this way, the variables $\lambda_i, i\in\mathcal{I}$ will approach the same value. The last term of equation (17) is an innovation term. We explain the rationale behind this term by interpreting the estimation of the global power mismatch $\zeta_i(k)$ as the global net demand estimated by agent i at iteration k. If there is a net demand, agent i expects the cost of electricity to increase, since more incentives are needed to encourage more generation, and vice versa. According to the sub-problems (10), as the price estimation λ_i increases, the power generation of a generator will monotonically increase until its upper bound is reached, while the power consumption of a flexible load will monotonically decrease until the lower bound is reached. According to equation (19), $\Delta P_i(k)$ will be negative, causing power mismatch estimation ζ_i to approach zero when it is updated with equation (18). Therefore, Algorithm 1 iterates to a stationary point, where the price estimations reach a consensus value and the power mismatch estimations reach zero, i.e., $\lambda_i = \lambda^*, \zeta_i = 0, \forall i\in\mathcal{I}$, which will be theoretically proven later. The first difference between the proposed method and those in References [13], [18], [19] is that we allow the agents to select their initial states from given ranges, instead of given values. Compared with References [13], [18], our method is applied to a time-varying communication topology, and thus the weight matrices are designed to change dynamically. Compared with References [18], [19], our method further considers RESs and flexible loads in microgrids, which constructs a more general practical scenario.

B. Proof of Algorithm Convergence and Optimality

To analyze the convergence of the algorithm, we first reformulate the update rules (17) and (18) into the matrix form:

$$\begin{aligned}\begin{bmatrix} \boldsymbol{\lambda}\left(k+1\right) \\ \boldsymbol{\zeta}\left(k+1\right) \end{bmatrix} = &\begin{bmatrix} \boldsymbol{W}\left(k\right) & \eta\left(k\right)\boldsymbol{I} \\ \boldsymbol{0} & \boldsymbol{B}\left(k\right) \end{bmatrix}\begin{bmatrix} \boldsymbol{\lambda}\left(k\right) \\ \boldsymbol{\zeta}\left(k\right) \end{bmatrix} \\ &+ \begin{bmatrix} \boldsymbol{0} \\ \Delta\boldsymbol{P}\left(k\right) \end{bmatrix},\end{aligned} \tag{21}$$

where $\boldsymbol{I}$ is the identity matrix. The matrix form (21) is a linear non-homogeneous system, whose convergence is difficult to prove. However, the convergence of a linear homogeneous system can be analyzed with mathematical tools such as eigenvalue derivatives [39]. Thus, based on Theorem 1, we convert (21) to its homogeneous form.

Algorithm 1 Proposed Consensus-Based Algorithm

Initialization:

The initial power generation/consumption $P_i(0)$ can be set to any value within the range $\left[P_i^{\min}, P_i^{\max}\right]$. The consensus variables are initialized as follows:

$$\lambda_i(0) = \begin{cases} 0, & \forall i \in \mathcal{I}_{\mathrm{R}} \\ C_i'(P_i(0)), & \forall i \in \mathcal{I}_{\mathrm{G}} \\ U_i'(P_i(0)), & \forall i \in \mathcal{I}_{\mathrm{L}} \end{cases}, \tag{15}$$

$$\zeta_i(0) = \begin{cases} -P_i(0), & \forall i \in \mathcal{I}_{\mathrm{R}} \cup \mathcal{I}_{\mathrm{G}} \\ P_i(0), & \forall i \in \mathcal{I}_{\mathrm{L}} \end{cases}, \tag{16}$$

where $C_i'(\cdot)$ and $U_i'(\cdot)$ are the first-order derivatives of $C_i(\cdot)$ and $U_i(\cdot)$, respectively.

Iteration:

Step 1 **(Update price estimation):** Update λ_i as follows:

$$\begin{aligned}\lambda_i(k+1) =& \lambda_i(k) + \sum_{j \in \mathcal{N}_i^+(k)} w_{ij}(k)\left(\lambda_j(k) - \lambda_i(k)\right) \\ &+ \eta(k)\,\zeta_i(k),\end{aligned} \tag{17}$$

where $\eta(k)$ is the step size of using the power mismatch estimation to update the price estimation.

Step 2 **(Optimal response):** Each agent calculates its optimal response to $\lambda_i(k+1)$ according to equation (10).

Step 3 **(Update power mismatch estimation):** Update ζ_i as follows:

$$\begin{aligned}\zeta_i(k+1) =& \left(1 - \sum_{h \in \mathcal{N}_i^-(k)} b_{ih}(k)\right)\zeta_i(k) \\ &+ \sum_{j \in \mathcal{N}_i^+(k)} b_{ji}(k)\,\zeta_j(k) + \Delta P_i(k),\end{aligned} \tag{18}$$

where $\Delta P_i(k)$ is the change of the power resulting from the optimal response to the updated price, which is defined as

$$\Delta P_i(k) = \begin{cases} P_i(k) - P_i(k+1), \forall i \in \mathcal{I}_{\mathrm{R}} \cup \mathcal{I}_{\mathrm{G}} \\ P_i(k+1) - P_i(k), \forall i \in \mathcal{I}_{\mathrm{L}} \end{cases}. \tag{19}$$

Step 4 **(Termination check):** The algorithm is terminated if consensus variables λ_i and ζ_i reach a stationary point. Given the thresholds ϵ_λ and ϵ_ζ, the algorithm terminates if

$$\begin{cases} \|\lambda_i(k+1) - \lambda_i(k)\| \le \epsilon_\lambda \\ \|\zeta_i(k+1) - \zeta_i(k)\| \le \epsilon_\zeta \end{cases}. \tag{20}$$

Otherwise, let $k = k+1$ and go back to ***Step 1***.

Theorem 1. *By taking a small enough step size $\eta(k)$, the linear non-homogeneous system (21) can be well-approximated by the following linear homogeneous system:*

$$\begin{bmatrix} \boldsymbol{\lambda}(k+1) \\ \boldsymbol{\zeta}(k+1) \end{bmatrix} = \boldsymbol{T}(k) \begin{bmatrix} \boldsymbol{\lambda}(k) \\ \boldsymbol{\zeta}(k) \end{bmatrix},$$
$$\boldsymbol{T}(k) = \begin{bmatrix} \boldsymbol{W}(k) & \eta(k)\boldsymbol{I} \\ \boldsymbol{K}(k)\left(\boldsymbol{W}(k) - \boldsymbol{I}\right) & \boldsymbol{B}(k) + \eta(k)\boldsymbol{K}(k) \end{bmatrix}, \tag{22}$$

where $\boldsymbol{K}(k)$ is a coefficient matrix, whose definition is presented in Appendix A.

Proof. Please see Appendix A. ■

Given the linear homogeneous system (22), we first discuss its stationary point. Recall that in equation (17), we define $\lambda_i(k+1)$ as the sum of the weighted average of $\lambda_j, \forall j \in \mathcal{N}_i^+(k) \cup \{i\}$ and a portion of $\zeta_i(k)$. Therefore, for every i, $\lambda_i(k+1) = \lambda_i(k)$ holds if and only if $\lambda_i(k) = \lambda_j(k), \forall j \in \mathcal{N}_i^+(k)$ and $\zeta_i(k) = 0$. Thus, as equation (22) converges to an equilibrium, $\boldsymbol{\lambda}(k)$ and $\boldsymbol{\zeta}(k)$ converge to $\lambda^*\mathbf{1}$ and $\mathbf{0}$, respectively. Hence, $\begin{bmatrix}\lambda^*\mathbf{1}^{\mathrm{T}} & \mathbf{0}^{\mathrm{T}}\end{bmatrix}$ is the target equilibrium state of system (22). Considering that the linear homogeneous system (22) is time varying, we introduce two probabilistic descriptions of convergence, which are defined as follows:

Definition 1 (*Mean square* consensus [40])**.** *For system (22), the mean square consensus is achieved if $E\left[\|\boldsymbol{\lambda}(k) - \lambda^*\mathbf{1}\|_2^2\right] \to 0$ and $E\left[\|\boldsymbol{\zeta}(k) - \mathbf{0}\|_2^2\right] \to 0$ hold as $k \to \infty$ for every initialization following equations (15) and (16).*

Definition 2 (*Almost sure* consensus [40])**.** *For system (22), the almost sure consensus is achieved if $\begin{bmatrix}\boldsymbol{\lambda}^T & \boldsymbol{\zeta}^T\end{bmatrix} \to \begin{bmatrix}\lambda^*\mathbf{1}^T & \mathbf{0}^T\end{bmatrix}$ as $k \to \infty$ with probability 1, for every initialization following equations (15) and (16).*

The convergence of the algorithm and the optimality of the obtained solution are stated through the following theorems.

Theorem 2. *With a small enough step size $\eta(k)$ at every iteration, the mean square consensus of system (22) is achieved by Algorithm 1.*

Proof. Please see Appendix B. ■

Theorem 3. *If Algorithm 1 achieves the mean square consensus of system (22), then $\begin{bmatrix}\boldsymbol{\lambda}^T & \boldsymbol{\zeta}^T\end{bmatrix}$ converges to $\begin{bmatrix}\lambda^*\mathbf{1}^T & \mathbf{0}^T\end{bmatrix}$ with probability 1.*

Proof. Please see Appendix C. ■

Theorem 4. *If there exists a feasible solution to problem (7), the stationary point of system (22) that Algorithm 1 converges to is the global optimal solution of problem (7).*

Proof. Please see Appendix D. ■

Remark. *Theorem 2 implies that for the linear homogeneous system (22), the expected value of the mean square error between its stationary point and the target equilibrium converges to zero as the algorithm iterates. Theorem 3 states that although the communication topology of the proposed method is random and time varying, the target equilibrium will eventually be reached as $k \to \infty$. Theorem 4 states the optimality of the solution obtained by Algorithm 1.*

IV. Case Study

In this section, we validate the effectiveness of the proposed method with multiple experiments, both within a simulation environment and on a hardware system. We first introduce

TABLE I
PARAMETERS OF AGENTS IN CASE STUDY

Agent	Type	q ($/MW^2)	l ($/MW)	$P^{\max}$ (MW)	$P^{\min}$ (MW)
1	Diesel generator	0.4	0	7	0
2	Diesel generator	0.6	0	6	0
3	RES	-	-	4.2	0
4	Flexible load	−2.5	30	6	4.5
5	Flexible load	−2.8	44.8	8	6
6	Flexible load	−3	48	8	5.8
7	Diesel generator	0.5	0	5	0

the setup of the blockchain-empowered energy management system and the parameters of the microgrid system. With these systems, we demonstrate that if the communication topology is time invariant and known, malicious agents can mislead the decision of an innocent agent. We also demonstrate that the proposed method converges to the global optimal solution as collusion is prevented. The plug-and-play capability of the proposed algorithm is tested in case 2, where an agent plugs in later than the others. In case 3, we test the proposed algorithm in a modified 51-bus distribution system [41], and we show that the convergence time of the proposed algorithm did not significantly increase as the number of agents increased.

A. System Setup

1) Hardware system: To evaluate the feasibility of the proposed method, we set up the blockchain-empowered energy management system on seven Rock Pi X devices, as shown in Fig. 2a. Rock Pi X is an X86 single-board computer, which features a 64-bit Intel Cherry Trail quad-core processor Atom x5-Z8350, 4 GB of RAM, and a 32-GB SD card. All of the Rock Pi X devices ran Ubuntu 20.04 as the operating system [42]. The communication network between Rock Pi X devices was established based on the gRPC framework with the Go programming language [43].

2) Blockchain system: In this study, we adopted an open-source blockchain platform, Hyperledger Fabric, to deploy our proposed blockchain framework. Specifically, we used Hyperledger Fabric v2.3, for the following reasons. First, this is a long-term support release that has been well verified. Second, Hyperledger Fabric supports smart contracts, which are essential to the implementation of our proposed method. Third, the smart contract of the Hyperledger Fabric can be written in standard programming languages, e.g., Go and JavaScript, which makes it easy for us to realize our customized designs.

In the blockchain network, each Rock Pi X device served as a peer node and represented one agent in the microgrid. As a permissioned blockchain, a digital identity, which was encapsulated in an X.509 digital certificate, was assigned to each agent in the microgrid. The X.509 certificate was stored in the corresponding Rock Pi X device and used for the authenticity check when the agent interacted with the blockchain. We also used a web-based front-end utility to visualize the activities of the proposed blockchain framework, as shown in Fig. 2b.

3) Microgrid system: The microgrid system used in cases 1 and 2 had seven agents, including three diesel generators, one RES, and three flexible loads. The parameters of the agents are outlined in Table I. We adopted a modified 51-bus distribution system in case 3, the parameters of which are outlined in Table V. During the solution process, at each iteration, each agent accessed its corresponding peer node in the blockchain network to exchange information with other agents. Then, each agent executed Steps 1–4 of Algorithm 1 locally. We developed a terminal-based interface to show the solution process and the obtained solution of each agent, as shown in Fig. 2b.

B. Case 1: Effectiveness of Proposed Algorithm

In this case, the performances of the following methods were compared:

1) B1: The centralized optimization method, which provided the global optimal solution P_i^*.
2) B2: The conventional consensus-based method, which adopted the time-invariant communication topology in Fig. 3 and was vulnerable to collusion.
3) B3: The proposed consensus-based method, which adopted a time-varying communication topology empowered by the blockchain smart contract.

To measure the optimal gap during the iteration process, the Euclidean distance to the global optimum is defined as

$$\delta_k = \|\boldsymbol{P}_k - \boldsymbol{P}^*\|. \tag{23}$$

To indicate the accuracy of the final solutions obtained by B2 and B3, we also define the percentage difference of the power compared with the results of B1:

$$\rho_i = \frac{(P_i - P_i^*)}{P_i^*}, \tag{24}$$

where ρ_i is the percentage difference of the power, P_i is the final solution, and P_i^* is the global optimal solution obtained by B1.

To show the impact of collusion on the social welfare, we define the welfare of each agent and its corresponding percentage difference as

$$\pi_i = \begin{cases} \lambda P_i, & \forall i \in \mathcal{I}_{\mathrm{R}}, \\ \lambda P_i - C_i(P_i), & \forall i \in \mathcal{I}_{\mathrm{G}}, \\ U_i(P_i) - \lambda P_i, & \forall i \in \mathcal{I}_{\mathrm{L}}, \end{cases} \tag{25}$$

$$\varrho_i = \frac{(\pi_i - \pi_i^*)}{\pi_i^*}, \tag{26}$$

where π_i is the welfare of agent i, ϱ_i is the percentage difference corresponding to π_i, and π_i^* is the global optimal solution obtained by B1. Thus, the social welfare of the microgrid system can be expressed as $\pi = \sum_{i\in\mathcal{I}} \pi_i$.

The results of these three methods are listed in Tables II and III. The iteration processes of the different variables are shown in Fig. 4. For both B2 and B3, the global power mismatch $\zeta = 0$, implying that the obtained solutions were both feasible. However, as B2 adopted time-invariant communication, malicious agents (Agents 2 and 3) could mislead the victim (Agent 7) into believing that the electricity price was converging to zero, as shown by the dashed line in Fig. 4c. Following

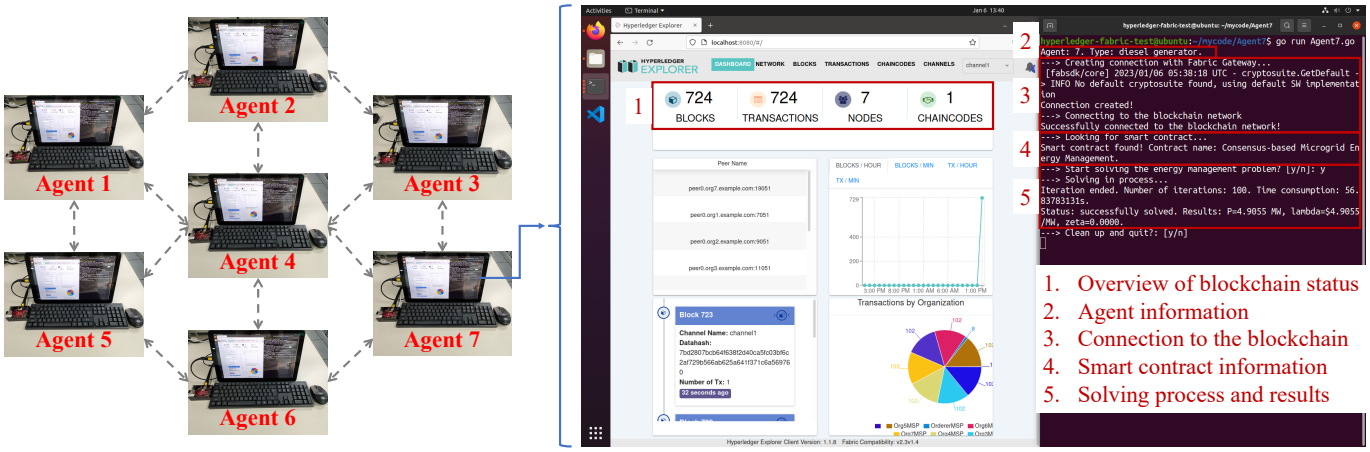

(a) Hardware system based on Rock Pi X devices

(b) Web-based visualization and terminal-based interface

Fig. 2. Hardware experiment system based on Rock Pi X devices, a web-based visualization of the blockchain, and a terminal-based interface.

TABLE II
RESULTS OF CASE 1: POWER

	P_1(MW)	P_2(MW)	P_3(MW)	P_4(MW)	P_5(MW)	P_6(MW)	P_7(MW)	ζ(MW)
B1	6.1319	4.0879	4.2000	5.0189	7.1240	7.1824	4.9055	0.0000
B2	8.4647	5.6431	4.2000	4.6457	6.7908	6.8714	0.0000	0.0000
B3	6.1319	4.0879	4.2000	5.0189	7.1240	7.1824	4.9055	0.0000
ρ^{B2}	+38.04%	+38.04%	0	−7.44%	−4.68%	−4.33%	−100.00%	0
ρ^{B3}	0	0	0	0	0	0	0	0

TABLE III
RESULTS OF CASE 1: WELFARE

	π_1($)	π_2($)	π_3($)	π_4($)	π_5($)	π_6($)	π_7($)	λ($/MWh)	π($)
B1	15.0400	10.0267	20.6031	62.9733	142.1045	154.7612	12.0320	4.9055	417.5409
B2	28.6603	19.1069	28.4413	53.9552	129.1204	141.6475	0.0000	6.7717	400.9315
B3	15.0400	10.0267	20.6031	62.9733	142.1045	154.7612	12.0320	4.9055	417.5409
ϱ^{B2}	+90.56%	+90.56%	+38.04%	−14.32%	−9.14%	−8.47%	−100.00%	+38.04%	−3.98%
ϱ^{B3}	0	0	0	0	0	0	0	0	0

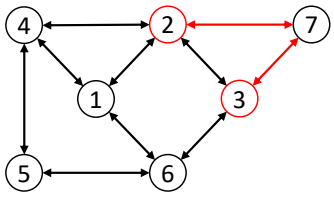

Fig. 3. Time-invariant communication topology used in case 1, where malicious agents (Agents 2 and 3) can block an innocent agent (Agent 7) out of the solution process.

equation (10), Agent 7 did not generate electricity, which resulted in a 38.04% increase in the electricity price. The generation of the malicious agents also increased, leading to a significant increase in the welfare of Agents 2 and 3. However, the welfare of all the agents on the demand side and the victim, i.e., Agent 7, was reduced due to the collusion of Agents 2 and 3. Such collusion also led to a 3.98% decrease in the social welfare of the entire microgrid. Since the proposed method adopted a time-varying communication topology empowered by a blockchain smart contract, the malicious agents could not send manipulated information to the victim, i.e., the collusion was prevented. The solution obtained by the proposed method was identical to the global optimal solution, which verified its effectiveness.

C. Case 2: Plug-and-Play Capability

In case 2, to test the plug-and-play capability, it was assumed that Agent 7 plugged in later than the other agents. The optimal solutions in two scenarios, i.e., the microgrid with and without Agent 7, are outlined in Table IV. Agents 1–6 first tried to solve the energy management problem. As shown in Fig. 5, Agents 1–6 converged to the original optimal solution until Agent 7 plugged in at the 50th iteration. As the optimal solution changed, each agent adjusted its power generation accordingly. Without requiring a re-initialization of the solution process, the system converged to the new optimal solution quickly. This implied that the proposed algorithm has plug-and-play capabilities.

TABLE IV
RESULTS OF DIFFERENT SCENARIOS IN CASE 2

Scenario	P_1^*(MW)	P_2^*(MW)	P_3^*(MW)	P_4^*(MW)	P_5^*(MW)	P_6^*(MW)	P_7^*(MW)	λ^*($/MWh)
w/o Agent 7	8.4647	5.6431	4.2000	4.6457	6.7908	6.8714	-	6.7717
w/ Agent 7	6.1319	4.0879	4.2000	5.0189	7.1240	7.1824	4.9055	4.905

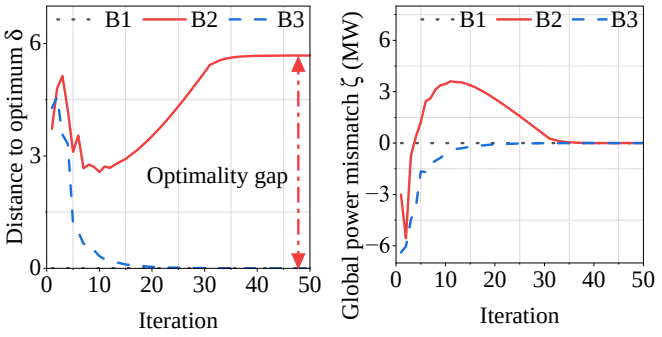

(a) Euclidean distance to optimum (b) Global power mismatch

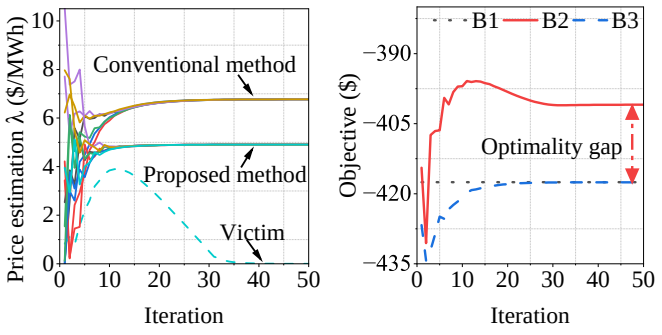

(c) Price estimation (d) Value of objective function

Fig. 4. Results of case 1: a) Euclidean distance to optimum, b) global power mismatch, c) price estimation, and d) value of the objective function. In the presence of malicious agents, the consensus-based algorithm on the time-invariant topology converged to a non-optimal but feasible solution. The proposed method converged to the global optimal solution since collusion was prevented.

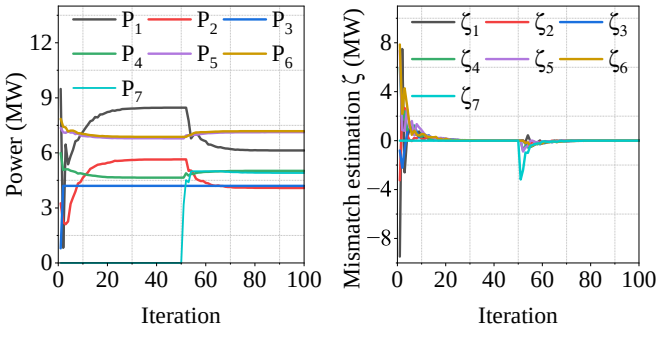

(a) Power generation/consumption (b) Power mismatch estimation

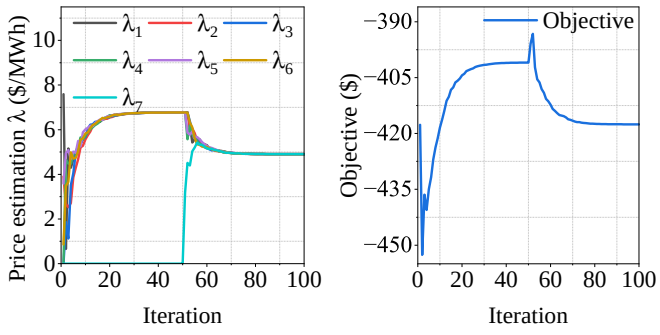

(c) Price estimation (d) Value of objective function

Fig. 5. Results of case 2: a) Power generation/consumption, b) power mismatch estimation, c) price estimation, and d) value of the objective function. The variables first converged to the global optimum of the energy management problem with six agents. After Agent 7 plugged in, the variables converged to a new equilibrium that coincided with the optimal solution of the current scenario, without requiring a re-initialization of the solution process.

D. Case 3: 51-bus Distribution System Implementation

The proposed consensus-based energy management algorithm was tested on a modified 51-bus distribution system. As shown in Fig. 6, the generation side consisted of seven diesel generators and five RESs, with overall capacities of 50 and 25 MW, respectively. Denoted by the orange arrows, there existed six flexible loads in the system, for which the power consumption could range from 18.75 to 25 MW in total. The rest of the loads were non-dispatchable critical loads, which were aggregated by five aggregators in the energy management problem, consuming 25 MW of power in total. The parameters of each agent are listed in Table V.

The results of case 3 are listed in Table VI. As illustrated in Fig. 7a, within 50 iterations, the power generation/consumption of each agent converged to the stationary point, which coincided with the results from a centralized optimization solver. As shown in Fig. 7b, the power mismatch estimations of all of the agents were reduced to zero, implying that the global power balance constraint (7b) was satisfied. Thus, the obtained solution was a feasible solution to the microgrid energy management problem. Illustrated by Fig. 7c, the price estimation of each agent converged to $3.1240/MWh, which was identical to the optimal value of the dual variable provided by the centralized method. The value of the objective function (7a) also converged to the optimal point, as shown in Fig. 7d. This case demonstrated that the iterations needed by the proposed method to reach the global optimum did not significantly increase as the number of agents increased. Thus, the proposed method has great potential to be applied in large-scale systems.

V. CONCLUSIONS

To promote the local accommodation of renewable energy, in this paper, we propose a blockchain-empowered framework for microgrid energy management. The energy management problem was formulated into a convex and decomposable form, and consequently it could be solved in a decentralized manner. Considering the prevention of collusion between

TABLE V
PARAMETERS OF AGENTS IN CASE 3

Agent	Type	q ($/MW^2)	l ($/MW)	P^{max} (MW)	P^{min} (MW)
1	Diesel generator	0.4	0	10	0
2	Diesel generator	0.6	0	6.5	0
3	Diesel generator	0.5	0	9.5	0
4	Diesel generator	0.7	0	5	0
5	Diesel generator	0.43	0	8.5	0
6	Diesel generator	0.48	0	5.5	0
7	Diesel generator	0.56	0	5	0
8	RES	-	-	7	0
9	RES	-	-	3.25	0
10	RES	-	-	5	0
11	RES	-	-	6	0
12	RES	-	-	3.75	0
13	Flexible load	−2.5	25	5	3.75
14	Flexible load	−2.8	19.6	3.5	2.25
15	Flexible load	−3	34.5	5.75	4.5
16	Flexible load	−2.2	17.6	4	2.75
17	Flexible load	−2.6	19.5	3.75	3
18	Flexible load	−3.5	21	3	2.5
19	Fixed load	−3	30	5	5
20	Fixed load	−3.2	35.2	5.5	5.5
21	Fixed load	−3.5	43.75	6.25	6.25
22	Fixed load	−2.9	26.1	4.5	4.5
23	Fixed load	−3.1	23.25	3.75	3.75

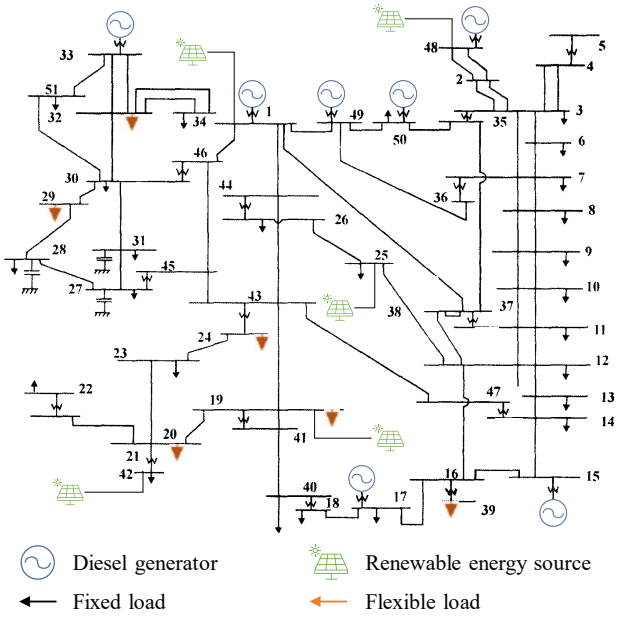

Fig. 6. 51-bus distribution system with seven generators, five renewable energy sources, and six flexible loads.

malicious agents, we propose a random information transmission mechanism to replace the time-invariant communication topology and integrate it into the smart contract of the proposed blockchain framework. To tackle the challenges brought by the time-varying communication topology, we adopt a novel consensus-based algorithm to obtain the optimal solution of the energy management problem. Beyond the numerical demonstration, the convergence of the algorithm and the optimality of the solution were theoretically proven. In the case studies, we demonstrated that the conventional method is prone to collusion, while the proposed method

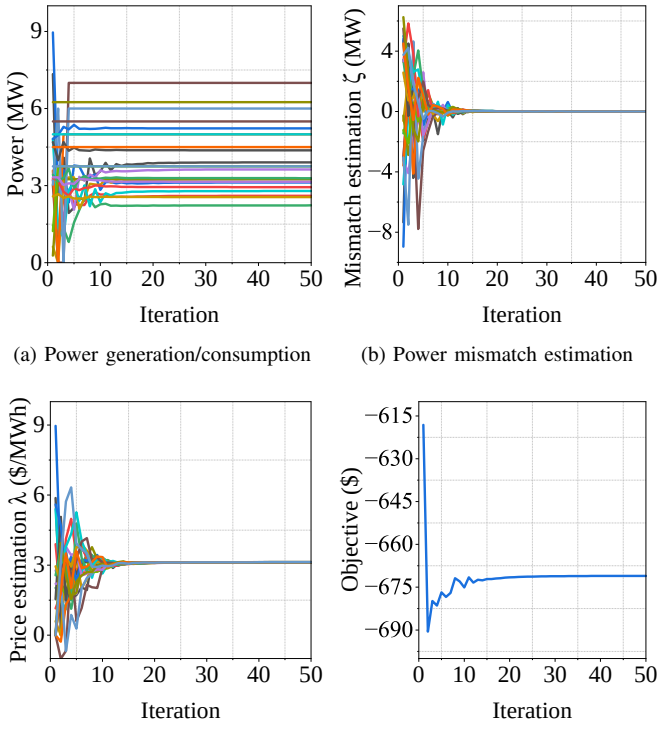

(a) Power generation/consumption (b) Power mismatch estimation

(c) Price estimation (d) Value of objective function

Fig. 7. Results of case 3: a) Power generation/consumption, b) power mismatch estimation, c) price estimation, and d) value of the objective function. The variables gradually converged to the global optimal solution of the energy management problem, without a significant increase in the convergence time, which demonstrates the capability of the proposed algorithm on a large system.

can obtain the global optimal solution. In addition to the convergence and optimality, the plug-and-play capability of the proposed algorithm was also verified, as the proposed method did not require re-initialization after new agents plugged in. The proposed algorithm was also implemented in a modified 51-bus distribution system to show that the solution time did not significantly increase as the size of the system increased. To keep the mathematical formulation clear and easy to understand, the power transfer loss of the microgrid was not considered in this paper. Future research directions might include modeling the power transfer loss in the energy management problem to make the power balance of the microgrid more precise.

APPENDIX A
PROOF OF THEOREM 1

To derive the homogeneous form of (21), we first introduce the following lemma.

Lemma 1 (Linear approximation [19])**.** *With a small enough step size $\eta(k)$ at every iteration k, the solution of sub-problems (10) can be well-approximated through linearization.*

For $i \in \mathcal{I}_G$, the first order optimality condition of (10) is

$$\lambda_i(k) = C_i'(P_i(k)), \tag{27}$$

where $C_i'(\cdot)$ is the first-order derivative of the cost function with respect to P_i.

TABLE VI
RESULTS OF CASE 3

P_1^*(MW)	P_2^*(MW)	P_3^*(MW)	P_4^*(MW)	P_5^*(MW)	P_6^*(MW)	P_7^*(MW)	P_8^*(MW)
3.9050	2.6033	3.1240	2.2314	3.6325	3.2541	2.7893	7.0000
P_9^*(MW)	P_{10}^*(MW)	P_{11}^*(MW)	P_{12}^*(MW)	P_{13}^*(MW)	P_{14}^*(MW)	P_{15}^*(MW)	P_{16}^*(MW)
3.2500	5.0000	6.0000	3.7500	4.3752	2.9421	5.2293	3.2900
P_{17}^*(MW)	P_{18}^*(MW)	P_{19}^*(MW)	P_{20}^*(MW)	P_{21}^*(MW)	P_{22}^*(MW)	P_{23}^*(MW)	λ^*($/MWh)
3.1492	2.5537	5.0000	5.5000	6.2500	4.5000	3.7500	3.1240

Lemma 1 implies that by lifting the power limits, the following first-order Taylor expansion around a fixed point $P_i(k)$ holds:

$$\begin{aligned}\lambda_i(k)+\Delta\lambda_i(k)\approx C_i^{'}(P_i(k))+C_i^{''}(P_i(k))\Delta P_i(k)\\ \Rightarrow \Delta P_i(k)\approx\left[C_i^{''}(P_i(k))\right]^{-1}\Delta\lambda_i(k).\end{aligned}\quad(28)$$

Considering the power limits, at iteration $k+1$, the power generation of the diesel generator can be expressed as

$$\begin{aligned}P_i(k+1)=&P_i(k)-K_i(k)\left(\lambda_i(k+1)-\lambda_i(k)\right),\\ &-\left[C_i^{''}(P_i(k))\right]^{-1}<K_i(k)<0,\end{aligned}\quad(29)$$

where $K_i(k)$ is a coefficient that relates the change of power to the change of the price estimation at iteration k.

Based on equation (19), $\Delta P_i(k)$ can be rewritten as

$$\Delta P_i(k)=K_i(k)\left(\lambda_i(k+1)-\lambda_i(k)\right),\forall i\in\mathcal{I}_{\mathrm{G}}.\quad(30)$$

Similarly, for $i\in\mathcal{I}_{\mathrm{L}}$, the power consumption at iteration $k+1$ can be expressed as

$$\begin{aligned}P_i(k+1)=&P_i(k)+K_i(k)\left(\lambda_i(k+1)-\lambda_i(k)\right),\\ &\left[U_i^{''}(P_i(k))\right]^{-1}<K_i(k)<0,\end{aligned}\quad(31)$$

which implies that equation (30) holds for every $i\in\mathcal{I}_{\mathrm{L}}$.

For $i\in\mathcal{I}_{\mathrm{R}}$, equation (10) implies that

$$P_i(k+1)=P_i(k)=P_i^{\max}.\quad(32)$$

By assuming that $K_i(k)=0,\forall i\in\mathcal{I}_{\mathrm{R}}$, equation (30) also holds for every $i\in\mathcal{I}_{\mathrm{R}}$. Thus, by taking $\boldsymbol{K}(k)=\mathrm{diag}\{K_i(k)\}$, the linear homogeneous form of system (21) can be written as

$$\begin{aligned}\begin{bmatrix}\boldsymbol{\lambda}(k+1)\\ \boldsymbol{\zeta}(k+1)\end{bmatrix}=\boldsymbol{T}(k)\begin{bmatrix}\boldsymbol{\lambda}(k)\\ \boldsymbol{\zeta}(k)\end{bmatrix},\\ \boldsymbol{T}(k)=\begin{bmatrix}\boldsymbol{W}(k) & \eta(k)\boldsymbol{I}\\ \boldsymbol{K}(k)\left(\boldsymbol{W}(k)-\boldsymbol{I}\right) & \boldsymbol{B}(k)+\eta(k)\boldsymbol{K}(k)\end{bmatrix}.\end{aligned}\quad(33)$$

APPENDIX B
PROOF OF THEOREM 2

For the linear homogeneous system (22), the matrix $\boldsymbol{T}(k)$ can be regarded as a matrix $\boldsymbol{T}_0(k)$ perturbed by $\eta(k)\boldsymbol{\Delta}(k)$ with the assumption of $\eta(k)$ being small enough, i.e.,

$$\boldsymbol{T}(k)=\boldsymbol{T}_0(k)+\eta(k)\boldsymbol{\Delta}(k),\quad(34)$$

where

$$\begin{cases}\boldsymbol{T}_0(k)=\begin{bmatrix}\boldsymbol{W}(k) & \boldsymbol{0}_{\mathrm{N}\times\mathrm{N}}\\ \boldsymbol{K}(k)\left(\boldsymbol{W}(k)-\boldsymbol{I}\right) & \boldsymbol{B}(k)\end{bmatrix}\\ \boldsymbol{\Delta}(k)=\begin{bmatrix}\boldsymbol{0}_{\mathrm{N}\times\mathrm{N}} & \boldsymbol{I}\\ \boldsymbol{0}_{\mathrm{N}\times\mathrm{N}} & \boldsymbol{K}(k)\end{bmatrix}\end{cases}.\quad(35)$$

Denoting the spectrum of a matrix by $E[\cdot]$, it holds that

$$E[\boldsymbol{T}(k)]=E[\boldsymbol{T}_0(k)]+\eta(k)E[\boldsymbol{\Delta}(k)].\quad(36)$$

Since $\boldsymbol{T}_0(k)$ is a lower triangular matrix, its eigenvalues are the eigenvalues of the matrices on the diagonal, i.e., $\boldsymbol{W}(k)$ and $\boldsymbol{B}(k)$. Since $\boldsymbol{W}(k)$ is a row stochastic matrix and $\boldsymbol{B}(k)$ is a column stochastic matrix, the eigenvalues of $\boldsymbol{T}_0(k)$ are

$$1=|\sigma_1|=|\sigma_2|>|\sigma_3|\ldots\geq|\sigma_{2\mathrm{N}}|.\quad(37)$$

Thus, 1 is the semi-simple eigenvalue, and the rest of the eigenvalues lie in the open unit disk of the complex plane. In the following paragraphs, we discuss the behavior of eigenvalues under a small perturbation $\eta(k)\boldsymbol{\Delta}(k)$.

For $\boldsymbol{T}_0(k)$, the right and left eigenvectors corresponding to eigenvalues σ_i by $\boldsymbol{\nu}_i$ and $\boldsymbol{\mu}_i$ are denoted as

$$\boldsymbol{\mu}_i^{\mathrm{T}}\boldsymbol{T}_0(k)=\sigma_i\boldsymbol{\mu}_i^{\mathrm{T}},\boldsymbol{T}_0(k)\boldsymbol{\nu}_i=\sigma_i\boldsymbol{\nu}_i,\boldsymbol{\mu}_i^{\mathrm{T}}\boldsymbol{\nu}_i=1,\boldsymbol{\mu}_i^{\mathrm{T}}\boldsymbol{\nu}_j=0.\quad(38)$$

It can be verified that the following vectors are the right and left eigenvectors corresponding to eigenvalues $\sigma_1=\sigma_2=1$ that satisfy equation (38):

$$\begin{cases}\begin{bmatrix}\boldsymbol{\nu}_1 & \boldsymbol{\nu}_2\end{bmatrix}=\begin{bmatrix}\boldsymbol{0} & \boldsymbol{1}\\ \frac{1}{\boldsymbol{1}^{\mathrm{T}}\boldsymbol{\gamma}_1}\boldsymbol{\gamma}_1 & \frac{\hat{K}(k)}{\boldsymbol{1}^{\mathrm{T}}\boldsymbol{\gamma}_1}\boldsymbol{\gamma}_1\end{bmatrix}\\ \begin{bmatrix}\boldsymbol{\mu}_1^{\mathrm{T}}\\ \boldsymbol{\mu}_2^{\mathrm{T}}\end{bmatrix}=\begin{bmatrix}-\boldsymbol{1}^{\mathrm{T}}\boldsymbol{K}(k) & \boldsymbol{1}^{\mathrm{T}}\\ \frac{1}{\boldsymbol{1}^{\mathrm{T}}\boldsymbol{\omega}_1}\boldsymbol{\omega}_1{}^{\mathrm{T}} & \boldsymbol{0}\end{bmatrix}\end{cases},\quad(39)$$

where γ_1 is the right eigenvector of $\boldsymbol{B}(k)$ corresponding to eigenvalue 1, ω_1 is the left eigenvector of $\boldsymbol{W}(k)$ corresponding to eigenvalue 1, and $\hat{K}(k)$ is defined as the sum of all $K_i(k)$ at iteration k, satisfying $\hat{K}(k)=\sum_{i\in\mathcal{I}}K_i(k)<0$.

According to the theory of eigenvalue derivatives [39], the derivative of the eigenvalues with respect to $\eta(k)$ at the point $\eta(k)=0$ can be calculated as

$$\frac{\partial\sigma_i}{\partial\eta(k)}=\boldsymbol{\mu}_i^{\mathrm{T}}\left.\frac{d\boldsymbol{T}(k)}{d\eta(k)}\right|_{\eta(k)=0}\boldsymbol{\nu}_i=\boldsymbol{\mu}_i^{\mathrm{T}}\boldsymbol{\Delta}(k)\boldsymbol{\nu}_i,\forall i\in\mathcal{I}.\quad(40)$$

The derivatives of $\sigma_1=1$ and $\sigma_2=1$ are

$$\frac{\partial\sigma_1}{\partial\eta(k)}=\begin{bmatrix}-\boldsymbol{1}^{\mathrm{T}}\boldsymbol{K}(k) & \boldsymbol{1}^{\mathrm{T}}\end{bmatrix}\boldsymbol{\Delta}(k)\begin{bmatrix}\boldsymbol{0}\\ \frac{1}{\boldsymbol{1}^{\mathrm{T}}\boldsymbol{\gamma}_1}\boldsymbol{\gamma}_1\end{bmatrix}=0,\quad(41)$$

$$\frac{\partial\sigma_2}{\partial\eta(k)}=\left[\frac{1}{\mathbf{1}^{\mathrm{T}}\boldsymbol{\omega}_1}\boldsymbol{\omega}_1{}^{\mathrm{T}}\quad\mathbf{0}^{\mathrm{T}}\right]\boldsymbol{\Delta}(k)\begin{bmatrix}\mathbf{1}\\ \frac{\hat{K}(k)}{\mathbf{1}^{\mathrm{T}}\boldsymbol{\gamma}_1}\boldsymbol{\gamma}_1\end{bmatrix}$$
$$=\frac{\hat{K}(k)}{\mathbf{1}^{\mathrm{T}}\boldsymbol{\omega}_1\cdot\mathbf{1}^{\mathrm{T}}\boldsymbol{\gamma}_1}\boldsymbol{\omega}_1{}^{\mathrm{T}}\boldsymbol{\gamma}_1<0. \tag{42}$$

Thus, there exists a small positive value $\epsilon_1>0$ such that the following equation holds if $\eta(k)<\epsilon_1$:

$$|\sigma_1|=1,\ |\sigma_2|<1. \tag{43}$$

Because the eigenvalues are continuous functions of matrix entries, there exists a small positive value $\epsilon_2>0$ such that the following equation holds if $\eta(k)<\epsilon_2$:

$$|\sigma_i|<|\sigma_2|<1. \tag{44}$$

With a small enough $\eta(k)$ such that $\eta(k)<\min(\epsilon_1,\epsilon_2)$, the eigenvalues of $E[\boldsymbol{T}(k)]$ satisfy

$$1=|\sigma_1|>|\sigma_2|>|\sigma_3|\ldots\geq|\sigma_{2\mathrm{N}}|. \tag{45}$$

Following Reference [19], we define the consensus error as

$$\boldsymbol{e}(k)=\begin{bmatrix}\boldsymbol{\lambda}(k)\\ \boldsymbol{\zeta}(k)\end{bmatrix}-\begin{bmatrix}\lambda^*\mathbf{1}\\ \mathbf{0}\end{bmatrix}. \tag{46}$$

The following equation holds since $\boldsymbol{W}(k)$ is a row stochastic matrix:

$$\boldsymbol{T}(k)\begin{bmatrix}\lambda^*\mathbf{1}\\ \mathbf{0}\end{bmatrix}=\begin{bmatrix}\lambda^*\mathbf{1}\\ \mathbf{0}\end{bmatrix}. \tag{47}$$

Then, one can infer that

$$\boldsymbol{e}(k+1)=\begin{bmatrix}\boldsymbol{\lambda}(k+1)\\ \boldsymbol{\zeta}(k+1)\end{bmatrix}-\begin{bmatrix}\lambda^*\mathbf{1}\\ \mathbf{0}\end{bmatrix}$$
$$=\boldsymbol{T}(k)\begin{bmatrix}\boldsymbol{\lambda}(k)\\ \boldsymbol{\zeta}(k)\end{bmatrix}-\boldsymbol{T}(k)\begin{bmatrix}\lambda^*\mathbf{1}\\ \mathbf{0}\end{bmatrix}=\boldsymbol{T}(k)\boldsymbol{e}(k). \tag{48}$$

Equation (48) implies that the evolution of $\boldsymbol{e}(k)$ can be described by the same linear system as equation (22). Defining a new vector $\mathring{\boldsymbol{e}}(k)\in\mathbb{R}^{4\mathrm{N}^2}$ as $\mathring{\boldsymbol{e}}(k)=\boldsymbol{e}(k)\otimes\boldsymbol{e}(k)$, where $\otimes$ is the Kronecker product, we can obtain

$$\begin{aligned}\mathring{\boldsymbol{e}}(k+1)&=\boldsymbol{e}(k+1)\otimes\boldsymbol{e}(k+1)\\&=(\boldsymbol{T}(k)\boldsymbol{e}(k))\otimes(\boldsymbol{T}(k)\boldsymbol{e}(k))\\&=(\boldsymbol{T}(k)\otimes\boldsymbol{T}(k))(\boldsymbol{e}(k)\otimes\boldsymbol{e}(k))\\&=(\boldsymbol{T}(k)\otimes\boldsymbol{T}(k))\,\mathring{\boldsymbol{e}}(k)\end{aligned}, \tag{49}$$

which implies that

$$E[\mathring{\boldsymbol{e}}(k+1)|\,\mathring{\boldsymbol{e}}(k)]=E[\boldsymbol{T}(k)\otimes\boldsymbol{T}(k)]\,\mathring{\boldsymbol{e}}(k). \tag{50}$$

Because the sequence $\{\boldsymbol{T}(k)\}$ is independent and identically distributed, the sequence $\{\boldsymbol{T}(k)\otimes\boldsymbol{T}(k)\}$ is independent and identically distributed. Then, equation (50) can be rewritten as

$$E[\mathring{\boldsymbol{e}}(k+1)|\,\mathring{\boldsymbol{e}}(k)]=E[\boldsymbol{T}\otimes\boldsymbol{T}]^k\,\mathring{\boldsymbol{e}}(0). \tag{51}$$

Lemma 2. *Assuming that matrix $\boldsymbol{A}\in\mathbb{R}^{n\times n}$ has $\alpha_1,\ldots,\alpha_n$ as its eigenvalues and matrix $\boldsymbol{B}\in\mathbb{R}^{m\times m}$ has $\beta_1,\ldots,\beta_m$ as its eigenvalues, the eigenvalues of $\boldsymbol{A}\otimes\boldsymbol{B}$ are $\alpha_i\beta_j\,(i=1,\ldots n,j=1,\ldots,m)$ [44].*

Lemma 2 implies that the eigenvalues of $E[\boldsymbol{T}\otimes\boldsymbol{T}]$ satisfy

$$1=|\varsigma_1|>|\varsigma_2|>|\varsigma_3|\ldots\geq|\varsigma_{4\mathrm{N}^2}|, \tag{52}$$

where ς_1 is the product of eigenvalue 1 of the matrix $\boldsymbol{T}$. According to Reference [45], the corresponding right and left eigenvectors corresponding to ς_1 are

$$\boldsymbol{r}_1=\boldsymbol{y}_1\otimes\boldsymbol{y}_1,\ \boldsymbol{l}_1^{\mathrm{T}}=\boldsymbol{z}_1^{\mathrm{T}}\otimes\boldsymbol{z}_1^{\mathrm{T}}, \tag{53}$$

where $\boldsymbol{y}_1$ and $\boldsymbol{z}_1$ are the right and left eigenvectors of $\boldsymbol{T}$ corresponding to eigenvalue 1, respectively, which have the following form:

$$\boldsymbol{y}_1=\begin{bmatrix}\mathbf{1}\\ \mathbf{0}\end{bmatrix},\ \boldsymbol{z}_1^{\mathrm{T}}=\frac{1}{\hat{K}(k)}\begin{bmatrix}\mathbf{1}^{\mathrm{T}}\boldsymbol{K} & -\mathbf{1}^{\mathrm{T}}\end{bmatrix}. \tag{54}$$

There exists a non-singular matrix $\boldsymbol{Q}$ such that

$$\boldsymbol{Q}^{-1}E[\boldsymbol{T}\otimes\boldsymbol{T}]\,\boldsymbol{Q}=\begin{bmatrix}1 & \mathbf{0}^{\mathrm{T}}\\ \mathbf{0} & \boldsymbol{J}\end{bmatrix}, \tag{55}$$

where $\boldsymbol{J}$ is the Jordan block matrix corresponding to the eigenvalues lying in the open unit disk. Thus, as $k\to\infty$,

$$E[\boldsymbol{T}\otimes\boldsymbol{T}]^k=\boldsymbol{Q}\begin{bmatrix}1 & \mathbf{0}^{\mathrm{T}}\\ \mathbf{0} & \boldsymbol{J}^k\end{bmatrix}\boldsymbol{Q}^{-1}\to\boldsymbol{r}_1\boldsymbol{l}_1^{\mathrm{T}}. \tag{56}$$

According to equation (54),

$$\boldsymbol{y}_1\boldsymbol{z}_1^{\mathrm{T}}=\frac{1}{\hat{K}(k)}\begin{bmatrix}\mathbf{1}\\ \mathbf{0}\end{bmatrix}\begin{bmatrix}\mathbf{1}^{\mathrm{T}}\boldsymbol{K} & -\mathbf{1}^{\mathrm{T}}\end{bmatrix}$$
$$=\frac{1}{\hat{K}(k)}\begin{bmatrix}\mathbf{1}_{\mathrm{N}\times\mathrm{N}}\boldsymbol{K} & -\mathbf{1}_{\mathrm{N}\times\mathrm{N}}\\ \mathbf{0}_{\mathrm{N}\times\mathrm{N}} & \mathbf{0}_{\mathrm{N}\times\mathrm{N}}\end{bmatrix}. \tag{57}$$

Based on the initialization rule (16), one can infer that

$$\begin{aligned}&\frac{1}{\hat{K}(k)}\begin{bmatrix}\mathbf{1}\mathbf{1}^{\mathrm{T}}\boldsymbol{K} & -\mathbf{1}\mathbf{1}^{\mathrm{T}}\\ \mathbf{0}\mathbf{0}^{\mathrm{T}} & \mathbf{0}\mathbf{0}^{\mathrm{T}}\end{bmatrix}\boldsymbol{e}(0)\\&=\frac{1}{\hat{K}(k)}\begin{bmatrix}\mathbf{1}\mathbf{1}^{\mathrm{T}}\boldsymbol{K} & -\mathbf{1}\mathbf{1}^{\mathrm{T}}\\ \mathbf{0}\mathbf{0}^{\mathrm{T}} & \mathbf{0}\mathbf{0}^{\mathrm{T}}\end{bmatrix}\left(\begin{bmatrix}\boldsymbol{\lambda}(0)\\ \boldsymbol{\zeta}(0)\end{bmatrix}-\begin{bmatrix}\lambda^*\mathbf{1}\\ \mathbf{0}\end{bmatrix}\right)\\&=\frac{1}{\hat{K}(k)}\begin{bmatrix}\mathbf{1}\mathbf{1}^{\mathrm{T}}\boldsymbol{K} & -\mathbf{1}\mathbf{1}^{\mathrm{T}}\\ \mathbf{0}\mathbf{0}^{\mathrm{T}} & \mathbf{0}\mathbf{0}^{\mathrm{T}}\end{bmatrix}\begin{bmatrix}\boldsymbol{\lambda}(0)\\ \boldsymbol{\zeta}(0)\end{bmatrix}\\&\quad-\frac{1}{\hat{K}(k)}\begin{bmatrix}\mathbf{1}\mathbf{1}^{\mathrm{T}}\boldsymbol{K} & -\mathbf{1}\mathbf{1}^{\mathrm{T}}\\ \mathbf{0}\mathbf{0}^{\mathrm{T}} & \mathbf{0}\mathbf{0}^{\mathrm{T}}\end{bmatrix}\begin{bmatrix}\lambda^*\mathbf{1}\\ \mathbf{0}\end{bmatrix}\\&=\frac{1}{\hat{K}(k)}\begin{bmatrix}\left(\sum_{i\in\mathcal{I}}P_i(0)-\sum_{i\in\mathcal{I}}\zeta_i(0)\right)\mathbf{1}\\ \mathbf{0}\end{bmatrix}\\&\quad-\frac{1}{\hat{K}(k)}\begin{bmatrix}\left(\sum_{i\in\mathcal{I}}P_i^*-\sum_{i\in\mathcal{I}}\zeta_i^*\right)\mathbf{1}\\ \mathbf{0}\end{bmatrix}=\begin{bmatrix}\mathbf{0}\\ \mathbf{0}\end{bmatrix}.\end{aligned} \tag{58}$$

Thus,

$$\begin{aligned}&E[\mathring{\boldsymbol{e}}(k+1)|\,\mathring{\boldsymbol{e}}(k)]\to r_1l_1^{\mathrm{T}}\mathring{\boldsymbol{e}}(0)\\&=\left(\frac{1}{\hat{K}(k)}\begin{bmatrix}\mathbf{1}\mathbf{1}^{\mathrm{T}}\boldsymbol{K} & -\mathbf{1}\mathbf{1}^{\mathrm{T}}\\ \mathbf{0}\mathbf{0}^{\mathrm{T}} & \mathbf{0}\mathbf{0}^{\mathrm{T}}\end{bmatrix}\otimes\frac{1}{\hat{K}(k)}\begin{bmatrix}\mathbf{1}\mathbf{1}^{\mathrm{T}}\boldsymbol{K} & -\mathbf{1}\mathbf{1}^{\mathrm{T}}\\ \mathbf{0}\mathbf{0}^{\mathrm{T}} & \mathbf{0}\mathbf{0}^{\mathrm{T}}\end{bmatrix}\right)\\&\quad\times\left(\left(\begin{bmatrix}\boldsymbol{\lambda}(0)\\ \boldsymbol{\zeta}(0)\end{bmatrix}-\begin{bmatrix}\lambda^*\mathbf{1}\\ \mathbf{0}\end{bmatrix}\right)\otimes\left(\begin{bmatrix}\boldsymbol{\lambda}(0)\\ \boldsymbol{\zeta}(0)\end{bmatrix}-\begin{bmatrix}\lambda^*\mathbf{1}\\ \mathbf{0}\end{bmatrix}\right)\right)\\&=\left(\frac{1}{\hat{K}(k)}\begin{bmatrix}\mathbf{1}\mathbf{1}^{\mathrm{T}}\boldsymbol{K} & -\mathbf{1}\mathbf{1}^{\mathrm{T}}\\ \mathbf{0}\mathbf{0}^{\mathrm{T}} & \mathbf{0}\mathbf{0}^{\mathrm{T}}\end{bmatrix}\left(\begin{bmatrix}\boldsymbol{\lambda}(0)\\ \boldsymbol{\zeta}(0)\end{bmatrix}-\begin{bmatrix}\lambda^*\mathbf{1}\\ \mathbf{0}\end{bmatrix}\right)\right)\\&\quad\otimes\left(\frac{1}{\hat{K}(k)}\begin{bmatrix}\mathbf{1}\mathbf{1}^{\mathrm{T}}\boldsymbol{K} & -\mathbf{1}\mathbf{1}^{\mathrm{T}}\\ \mathbf{0}\mathbf{0}^{\mathrm{T}} & \mathbf{0}\mathbf{0}^{\mathrm{T}}\end{bmatrix}\left(\begin{bmatrix}\boldsymbol{\lambda}(0)\\ \boldsymbol{\zeta}(0)\end{bmatrix}-\begin{bmatrix}\lambda^*\mathbf{1}\\ \mathbf{0}\end{bmatrix}\right)\right)\\&=\begin{bmatrix}\mathbf{0}\\ \mathbf{0}\end{bmatrix}\otimes\begin{bmatrix}\mathbf{0}\\ \mathbf{0}\end{bmatrix},\end{aligned} \tag{59}$$

implying that the expectation of the consensus error converges to zero, i.e., system (22) achieves mean square consensus. ■

APPENDIX C
PROOF OF THEOREM 3

Lemma 3. *For a discrete-time Markov jump linear system, it achieves almost sure consensus if it achieves mean square consensus [46].*

Based on Theorem 2, the system we studied achieves mean square consensus. Because the system is a discrete-time Markov jump linear system, Lemma 3 implies that the system achieves almost sure consensus. ■

APPENDIX D
PROOF OF OPTIMALITY

Since problem (7) is a convex optimization problem with affine constraints, proving Theorem 4 is equivalent to proving that the stationary point $[\boldsymbol{P}_i^*, \lambda^* \mathbf{1}, \mathbf{0}]$ satisfies the KKT conditions of problem (7).

We first prove that the equality constraint (7b) is satisfied at the stationary point. Recall that by definition (14), the matrix $\boldsymbol{B}(k)$ is a column stochastic matrix at each iteration k, i.e., the entries of each column of $\boldsymbol{B}(k)$ sum to 1. Thus, summing up both sides of equation (18) for all agents yields

$$\sum_{i\in\mathcal{I}} \zeta_i(k+1) = \sum_{i\in\mathcal{I}} \zeta_i(k) + \sum_{i\in\mathcal{I}} \Delta P_i(k). \tag{60}$$

According to equations (12) and (19), the following equation holds:

$$\sum_{i\in\mathcal{I}} \Delta P_i(k) = \zeta(k+1) - \zeta(k). \tag{61}$$

Substituting equation (61) into equation (60) yields

$$\sum_{i\in\mathcal{I}} \zeta_i(k+1) - \zeta(k+1) = \sum_{i\in\mathcal{I}} \zeta_i(k) - \zeta(k), \tag{62}$$

which holds for every k. Since the initialization rule (16) ensures that $\sum_{i\in\mathcal{I}} \zeta_i(0) - \zeta(0) = 0$, one can infer that

$$\sum_{i\in\mathcal{I}} \zeta_i(k) - \zeta(k) = 0, \tag{63}$$

implying that the global power mismatch equals zero as the algorithm converges, i.e., the equality constraint (7b) is satisfied. Since the satisfaction of constraint (7c) is guaranteed by (10), the stationary point $[\boldsymbol{P}_i^*, \lambda^* \mathbf{1}, \mathbf{0}]$ is a feasible solution to the primal problem (7).

The dual feasibility is proven by contradiction. Assuming that $\lambda^* < 0$, one can infer from equation (10) that $P_i = P_i^{\max}, \forall i \in \mathcal{I}_{\mathrm{L}}$ and $P_i = P_i^{\min}, \forall i \in \mathcal{I}_{\mathrm{R}} \cup \mathcal{I}_{\mathrm{G}}$. However, equation (8) implies that $\sum_{i\in\mathcal{I}_{\mathrm{R}}\cup\mathcal{I}_{\mathrm{G}}} P_i^{\min} < \sum_{i\in\mathcal{I}_{\mathrm{L}}} P_i^{\max}$, and thus, $\zeta \neq 0$, which is contradictory to the primal feasibility.

With the vector of KKT multipliers corresponding to the upper and lower limits of the power at the stationary point denoted by $\boldsymbol{\phi} = [\phi_1^*, \ldots, \phi_{\mathrm{N}}^*]^{\mathrm{T}}$ and $\boldsymbol{\xi} = [\xi_1^*, \ldots, \xi_{\mathrm{N}}^*]^{\mathrm{T}}$, the complementary slackness and stationary conditions are

$$\begin{cases} \phi_i^* \left(P_i - P_i^{\min}\right) = 0, & \forall i \in \mathcal{I}, \\ \xi_i^* \left(P_i^{\max} - P_i\right) = 0, & \forall i \in \mathcal{I}, \\ -\lambda^* + \phi_i^* - \xi_i^* = 0, & \forall i \in \mathcal{I}_{\mathrm{R}}, \\ C_i'(P_i^*) - \lambda^* + \phi_i^* - \xi_i^* = 0, & \forall i \in \mathcal{I}_{\mathrm{G}}, \\ -U_i'(P_i^*) + \lambda^* + \phi_i^* - \xi_i^* = 0, & \forall i \in \mathcal{I}_{\mathrm{L}}, \end{cases} \tag{64}$$

which can be satisfied by a proper selection of $\boldsymbol{\phi}$ and $\boldsymbol{\xi}$. ■

ACKNOWLEDGMENT

The authors would like to thank Dr. Yulin Chen for helping with checking the correctness of the mathematical proofs of this paper.

REFERENCES

[1] D. M. Kammen and D. A. Sunter, "City-integrated renewable energy for urban sustainability," *Science*, vol. 352, no. 6288, pp. 922–928, 2016.

[2] H. Sun, Q. Guo, J. Qi, V. Ajjarapu, R. Bravo, J. Chow, Z. Li, R. Moghe, E. Nasr-Azadani, U. Tamrakar, G. N. Taranto, R. Tonkoski, G. Valverde, Q. Wu, and G. Yang, "Review of challenges and research opportunities for voltage control in smart grids," *IEEE Transactions on Power Systems*, vol. 34, no. 4, pp. 2790–2801, 7 2019.

[3] H. Qiu, W. Gu, and F. You, "Bilayer distributed optimization for robust microgrid dispatch with coupled individual-collective profits," *IEEE Transactions on Sustainable Energy*, vol. 12, no. 3, pp. 1525–1538, 2021.

[4] P. Yu, H. Zhang, Y. Song, H. Hui, and G. Chen, "District Cooling System Control for Providing Operating Reserve Based on Safe Deep Reinforcement Learning," *IEEE Transactions on Power Systems*, pp. 1–13, 2023.

[5] H. Hui, P. Siano, Y. Ding, P. Yu, Y. Song, H. Zhang, and N. Dai, "A transactive energy framework for inverter-based HVAC loads in a real-time local electricity market considering distributed energy resources," *IEEE Transactions on Industrial Informatics*, vol. 18, no. 12, pp. 8409–8421, 12 2022.

[6] Z. Li, Z. Cheng, J. Liang, J. Si, L. Dong, and S. Li, "Distributed event-triggered secondary control for economic dispatch and frequency restoration control of droop-controlled AC microgrids," *IEEE Transactions on Sustainable Energy*, vol. 11, no. 3, pp. 1938–1950, 7 2020.

[7] H. Kanchev, F. Colas, V. Lazarov, and B. Francois, "Emission reduction and economical optimization of an urban microgrid operation including dispatched PV-based active generators," *IEEE Transactions on Sustainable Energy*, vol. 5, no. 4, pp. 1397–1405, 2014.

[8] A. Parisio, C. Wiezorek, T. Kyntäjä, J. Elo, K. Strunz, and K. H. Johansson, "Cooperative MPC-based energy management for networked microgrids," *IEEE Transactions on Smart Grid*, vol. 8, no. 6, pp. 3066–3074, 2017.

[9] J. Arkhangelski, M. Abdou-Tankari, and G. Lefebvre, "Day-ahead optimal power flow for efficient energy management of urban microgrid," *IEEE Transactions on Industry Applications*, vol. 57, no. 2, pp. 1285–1293, 2021.

[10] L. Du, S. Grijalva, and R. G. Harley, "Game-theoretic formulation of power dispatch with guaranteed convergence and prioritized best response," *IEEE Transactions on Sustainable Energy*, vol. 6, no. 1, pp. 51–59, 1 2015.

[11] Y. Chen, C. Li, D. Qi, Z. Li, Z. Wang, and J. Zhang, "Distributed event-triggered secondary control for islanded microgrids with proper trigger condition checking period," *IEEE Transactions on Smart Grid*, vol. 13, no. 2, pp. 837–848, 3 2022.

[12] N. Rahbari-Asr, U. Ojha, Z. Zhang, and M. Y. Chow, "Incremental welfare consensus algorithm for cooperative distributed generation/demand response in smart grid," *IEEE Transactions on Smart Grid*, vol. 5, no. 6, pp. 2836–2845, 2014.

[13] C. Zhao, J. He, P. Cheng, and J. Chen, "Consensus-based energy management in smart grid with transmission losses and directed communication," *IEEE Transactions on Smart Grid*, vol. 8, no. 5, pp. 2049–2061, 2017.

[14] C. Zhao, J. Chen, J. He, and P. Cheng, "Privacy-preserving consensus-based energy management in smart grids," *IEEE Transactions on Signal Processing*, vol. 66, no. 23, pp. 6162–6176, 2018.

[15] H. Hui, Y. Chen, S. Yang, H. Zhang, and T. Jiang, "Coordination control of distributed generators and load resources for frequency restoration in isolated urban microgrids," *Applied Energy*, vol. 327, no. August, p. 120116, 12 2022.

[16] W. Ananduta, C. Ocampo-Martinez, and A. Nedic, "A distributed augmented lagrangian method over stochastic networks for economic dispatch of large-scale energy systems," *IEEE Transactions on Sustainable Energy*, vol. 12, no. 4, pp. 1927–1934, 2021.

[17] J. Wu, T. Yang, D. Wu, K. Kalsi, and K. H. Johansson, "Distributed optimal dispatch of distributed energy resources over lossy communication networks," *IEEE Transactions on Smart Grid*, vol. 8, no. 6, pp. 3125–3137, 2017.

[18] D. Yang, S. Zhang, B. Zhou, and S. Bu, "Consensus-based decentralized optimization for distributed generators power allocation over time-varying digraphs in microgrids," *IEEE Systems Journal*, vol. 15, no. 1, pp. 814–825, 2021.

[19] R. Wang, Q. Li, G. Li, and H. Liu, "A gossip-based distributed algorithm for economic dispatch in smart grids with random communication link failures," *IEEE Transactions on Industrial Electronics*, vol. 67, no. 6, pp. 4635–4645, 2020.

[20] T. Zhao and Z. Ding, "Distributed agent consensus-based optimal resource management for microgrids," *IEEE Transactions on Sustainable Energy*, vol. 9, no. 1, pp. 443–452, 2018.

[21] Y. Zhou, A. N. Manea, W. Hua, J. Wu, W. Zhou, J. Yu, and S. Rahman, "Application of distributed ledger technology in distribution networks," *Proceedings of the IEEE*, pp. 1–13, 2022.

[22] S. Chen, H. Mi, J. Ping, Z. Yan, Z. Shen, X. Liu, N. Zhang, Q. Xia, and C. Kang, "A blockchain consensus mechanism that uses Proof of Solution to optimize energy dispatch and trading," *Nature Energy*, vol. 7, no. 6, pp. 495–502, 6 2022.

[23] X. Luo, K. Xue, J. Xu, Q. Sun, and Y. Zhang, "Blockchain based secure data aggregation and distributed power dispatching for microgrids," *IEEE Transactions on Smart Grid*, vol. 12, no. 6, pp. 5268–5279, 2021.

[24] Q. Yang and H. Wang, "Privacy-preserving transactive energy management for IoT-aided smart homes via blockchain," *IEEE Internet of Things Journal*, vol. 8, no. 14, pp. 11 463–11 475, 7 2021.

[25] F. Luo, Z. Y. Dong, G. Liang, J. Murata, and Z. Xu, "A distributed electricity trading system in active distribution networks based on multi-agent coalition and blockchain," *IEEE Transactions on Power Systems*, vol. 34, no. 5, pp. 4097–4108, 2019.

[26] M. L. Di Silvestre, P. Gallo, M. G. Ippolito, E. R. Sanseverino, and G. Zizzo, "A technical approach to the energy blockchain in microgrids," *IEEE Transactions on Industrial Informatics*, vol. 14, no. 11, pp. 4792–4803, 2018.

[27] G. van Leeuwen, T. AlSkaif, M. Gibescu, and W. van Sark, "An integrated blockchain-based energy management platform with bilateral trading for microgrid communities," *Applied Energy*, vol. 263, no. October 2019, p. 114613, 4 2020.

[28] Q. Yang, H. Wang, T. Wang, S. Zhang, X. Wu, and H. Wang, "Blockchain-based decentralized energy management platform for residential distributed energy resources in a virtual power plant," *Applied Energy*, vol. 294, no. December 2020, p. 117026, 2021.

[29] L. Yan, X. Chen, and Y. Chen, "A consensus-based privacy-preserving energy management strategy for microgrids with event-triggered scheme," *International Journal of Electrical Power and Energy Systems*, vol. 141, p. 108198, 2022.

[30] Y. Chen, D. Qi, H. Dong, C. Li, Z. Li, and J. Zhang, "A FDI attack-resilient distributed secondary control strategy for islanded microgrids," *IEEE Transactions on Smart Grid*, vol. 12, no. 3, pp. 1929–1938, 5 2021.

[31] C. Zhao, J. He, P. Cheng, and J. Chen, "Analysis of consensus-based distributed economic dispatch under stealthy attacks," *IEEE Transactions on Industrial Electronics*, vol. 64, no. 6, pp. 5107–5117, 2017.

[32] A. Kargarian, J. Mohammadi, J. Guo, S. Chakrabarti, M. Barati, G. Hug, S. Kar, and R. Baldick, "Toward distributed/decentralized DC optimal power flow implementation in future electric power systems," *IEEE Transactions on Smart Grid*, vol. 9, no. 4, pp. 2574–2594, 7 2018.

[33] S. Chen, Z. Shen, L. Zhang, Z. Yan, C. Li, N. Zhang, and J. Wu, "A trusted energy trading framework by marrying blockchain and optimization," *Advances in Applied Energy*, vol. 2, no. April, p. 100029, 5 2021.

[34] S. Chen, L. Zhang, Z. Yan, and Z. Shen, "A distributed and robust security-constrained economic dispatch algorithm based on blockchain," *IEEE Transactions on Power Systems*, vol. 37, no. 1, pp. 691–700, 1 2022.

[35] E. Androulaki, A. Barger, V. Bortnikov, C. Cachin, K. Christidis, A. De Caro, D. Enyeart, C. Ferris, G. Laventman, Y. Manevich, S. Muralidharan, C. Murthy, B. Nguyen, M. Sethi, G. Singh, K. Smith, A. Sorniotti, C. Stathakopoulou, M. Vukolić, S. W. Cocco, and J. Yellick, "Hyperledger fabric: a distributed operating system for permissioned blockchains," in *Proceedings of the Thirteenth EuroSys Conference*. New York, NY, USA: ACM, 4 2018, pp. 1–15.

[36] S. Yang, S. Tan, and J.-X. Xu, "Consensus based approach for economic dispatch problem in a smart grid," *IEEE Transactions on Power Systems*, vol. 28, no. 4, pp. 4416–4426, 2013.

[37] P. Samadi, H. Mohsenian-Rad, R. Schober, and V. W. Wong, "Advanced demand side management for the future smart grid using mechanism design," *IEEE Transactions on Smart Grid*, vol. 3, no. 3, pp. 1170–1180, 2012.

[38] G. C. Calafiore and L. El Ghaoui, *Optimization Models*. Cambridge University Press, 2014.

[39] N. Van der Aa, H. Ter Morsche, and R. Mattheij, "Computation of eigenvalue and eigenvector derivatives for a general complex-valued eigensystem," *The Electronic Journal of Linear Algebra*, vol. 16, no. October 2006, pp. 300–314, 2007.

[40] K. Cai and H. Ishii, "Average consensus on general strongly connected digraphs," *Automatica*, vol. 48, no. 11, pp. 2750–2761, 2012.

[41] P. Murty, *Power Systems Analysis*. BS Publications, 2007.

[42] Radxa Limited, "ROCK Pi X," 2023. [Online]. Available: https://wiki.radxa.com/RockpiX

[43] gRPC Authors, "Go—gRPC," 2022. [Online]. Available: https://grpc.io/docs/languages/go/

[44] J. Brewer, "Kronecker products and matrix calculus in system theory," *IEEE Transactions on Circuits and Systems*, vol. 25, no. 9, pp. 772–781, 1978.

[45] R. A. Horn and C. R. Johnson, *Topics in Matrix Analysis*. Cambridge University Press, 1991.

[46] O. L. V. do Costa, R. P. Marques, and M. D. Fragoso, *Discrete-Time Markov Jump Linear Systems*, ser. Probability and Its Applications. London: Springer London, 2005.

Hongyi Li (S'21) received the B.Eng. degree from Huazhong University of Science and Technology, Wuhan, China, in 2020 and the M.Sc. degree from Imperial College London, London, UK, in 2021, both in electrical engineering. He is currently working toward the Ph.D. degree at University of Macau, Macao, China. His research interests include Internet of Things for smart energy, consensus-based energy management and blockchain-assisted optimization technology.

Hongxun Hui (S'17–M'20) received the B.E. and Ph.D. degrees in electrical engineering from Zhejiang University, Hangzhou, China, in 2015 and 2020, respectively. He is currently a Research Assistant Professor with the State Key Laboratory of Internet of Things for Smart City, University of Macau, Macao SAR, China. From 2018 to 2019, he was a visiting scholar at the Advanced Research Institute in Virginia Tech, and the CURENT Center in University of Tennessee. His research interests include power system optimization, demand-side resource control, and Internet of Things technologies for smart energy.

Hongcai Zhang (S'14–M'18–SM'23) received the B.S. and Ph.D. degree in electrical engineering from Tsinghua University, Beijing, China, in 2013 and 2018, respectively. He is currently an Assistant Professor with the State Key Laboratory of Internet of Things for Smart City and Department of Electrical and Computer Engineering, University of Macau, Macao, China. In 2018-2019, he was a postdoctoral scholar with the Energy, Controls, and Applications Lab at University of California, Berkeley, where he also worked as a visiting student researcher in 2016. His current research interests include Internet of Things for smart energy, optimal operation and optimization of power and transportation systems, and grid integration of distributed energy resources.